Two-scale homogenization to determine effective parameters of thin metallic-structured films

Jean-Jacques Marigo, Agnès Maurel

rspa.royalsocietypublishing.org

Research

Article submitted to journal

Two scale homogenization to determine effective parameters of thin metallic structured films

Jean-Jacques Marigo and Agnès Maurel

Lab. Mécanique des Solides, CNRS, Ecole Polytechnique, Palaiseau, France
Institut Langevin, CNRS, ESPCI ParisTech, 1 rue Jussieu, 75005 Paris, France

We present a homogenization method based on matched asymptotic expansion technique to derive effective transmission conditions of thin structured films. The method leads unambiguously to effective parameters of the interface which define jump conditions or boundary conditions at an equivalent zero thickness interface. The homogenized interface model is presented in the context of electromagnetic waves for metallic inclusions associated to Neumann or Dirichlet boundary conditions for transverse electric (TE) or transverse magnetic (TM) wave polarization. By comparison with full wave simulations, the model is shown to be valid for thin interfaces up to thicknesses close to the wavelength. We also compare our effective conditions to the two-sided impedance conditions obtained in transmission line theory and to the so-called Generalized Sheet Transition Conditions (GSTCs).

1. Introduction

Metamaterial devices composed of a periodic arrangement of subwavelength unit cells have been widely studied using classical homogenization, see *e.g.* [1–3]. Owing to the resolution of so-called cell problems, written in the static limit, the problem ends with effective permeability and effective permittivity of an equivalent homogeneous medium (being possibly anisotropic). More recently, frequency dependences in the cell problems have been introduced, which allow to account for possible resonances in the unit cell; these are the high frequency homogenization or resonant homogenization [4–10]. However, the classical homogenization being developed for infinite media, its validity for devices of small thickness is questionable. This is because one has to impose an artificial, and arbitrary, thickness to the device and nowadays, it is admitted that an equivalent zero thickness interface is more adapted to describe the behavior of devices with subwavelength thickness [11,12]. The transmission line theory is accurate to that aim when the equivalent impedances of each component of the device are known [13,14]. Alternatively, Kuester, Holloway and coworkers have developed the so called "generalized sheet transition conditions" (GSTCs) [15–18], see also [19,20]. Although powerful, the transmission line theory and the GSTCs are predictive for particular cases only, and in general, the effective parameters have to be retrieved from the scattering coefficients. Thus, if the problem of the artificial thickness is avoided, the problem of whether or not the model imposed to the device is adapted remains. Finally, although more incidental, these methods cannot be extended easily to other contexts of wave propagation, even when the Helmholtz equation applies. Indeed, they are intimately related to the notion of charges and currents, which do not have natural counterparts in acoustics and in elasticity.

In this paper, we present an homogenization method for structured interfaces, or structured films, with vanishing thicknesses, based on matched asymptotic expansions of the solution of the Helmholtz equation. The problem ends with effective conditions at an equivalent zero thickness surface involving parameters being wave independent, by construction. This is because, as in the classical homogenization, the parameters are determined by solving (analytically or numerically) elementary problems in the static case (that is for zero frequency). This approach has been developed in the context of the static elasticity, see [21,22] for a complete description. The case of wave propagation has been less regarded. We mention the works of Capdeville and Marigo in the context of seismic waves [23–27], and similar works developed by the community of french applied mathematics in acoustics [28] and in electromagnetism [29,30]. Note also works using alternative forms of homogenizations [31–34].

The method, directly inspired by [21], is presented in Section 2 considering the Helmholtz equation for films composed of a periodic array of inclusions associated with Neumann or Dirichlet boundary conditions. In acoustics, this corresponds to sound hard or sound soft inclusions, respectively, and the method holds in three dimensions. In electromagnetism, the Helmholtz equation applies for waves being polarized; for a perfectly conducting metal, Neumann boundary conditions apply in transverse magnetic polarization (TM), and Dirichlet boundary conditions apply in transverse electric polarization (TE). It is shown that, at the dominant order, the wave does not see a film structured with Neumann inclusions and as a second order correction, jump conditions on the field and its normal derivatives are established, Eqs. (2.16). These jump conditions involve interface parameters (9 in three dimensions and 5 in two dimensions for non symmetrical inclusions), among which the surface (or volume) of the inclusions, and others, Eqs. (2.17), defined in the 3 elementary problems, Eqs. (2.13). The case of Dirichlet scatterers is very different. At the dominant order, the wave sees the array of scatterers as a perfectly reflecting wall. As a second order correction, we get boundary conditions for the electric fields on each side of the film, Eqs. (2.31); these boundary conditions involve 3 interface parameters defined in two elementary problems, Eqs. (2.28)-(2.30).

Validations of our homogenized interface model are presented in Section 3 in the case of an incident plane wave at oblique incidences on a film composed of a periodic array of rectangular

metallic inclusions in two dimensions. In TM and TE polarizations, the model is shown to be valid for a film thickness e smaller than the wavelength (with typical validity range $ke < 1$, and k is the free space wavenumber).

In Section 4, we compare the effective conditions given by our model with the so-called two-sided impedance conditions obtained in the transmission line model and with the generalized sheet transition conditions. Correspondances are obtained and discussed for simple geometries corresponding to a planar array of capacitive or inductive strips ($e \to 0$ and the inclusions occupy a large or a small fraction of the unit cell, for TM or TE polarizations, respectively).

In the Appendix, the robustness of the method is shown by comparing the effective parameters calculated in the elementary problems to those obtained by means of retrieval methods.

Throughout the paper, time dependence is $e^{-i\omega t}$, with ω the frequency and t the time. Also, for a function being discontinuous at 0, we use

$$\begin{cases} \bar{f}(0) \equiv \frac{1}{2}\left[f(0^+) + f(0^-)\right], \\ [\![f]\!] \equiv f(0^+) - f(0^-). \end{cases} \tag{1.1}$$

2. Homogenized interface model

We consider an array of inclusions, or scatterers, periodically located on a surface with spacing h, and thickness e, Fig. 1(a). The goal is to replace this structured interface by an equivalent zero thickness interface (Fig. 1(b)), associated to jump or boundary conditions, with the same scattering properties than the actual interface for any scattering problem. The model relies on a separation of scales, a micro scale associated to the small scatterer size and a macro scale associated to the wavelength, and ε is the small parameter that measures the ratio of the two scales. Each scale is associated to a system of coordinates which is relevant or not to describe the variations of the wavefields whether we are close to the film or far from it. Thus, a separation of the space is used, into an outer region, typically the far field, where only the macro scale makes sense and an inner region, the near field, where both the micro and the macro scales are needed. Expansions of the fields in power of ε are performed in both regions and finally, matching conditions are used between the two regions. These matching conditions are the boundary conditions for the outer solution and they encapsulate the effect of the inclusions in interface parameters which are wave independent by construction.

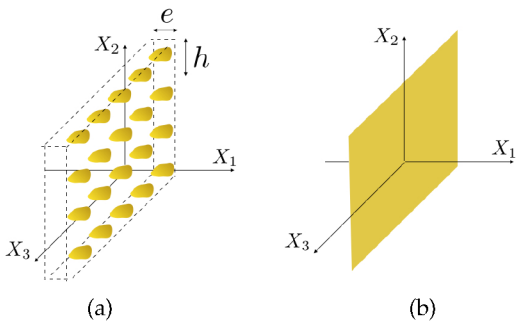

Figure 1. Typical configuration of (a) the actual microstructured film and (b) the equivalent zero thickness interface.

(a) Inclusions associated to Neumann boundary conditions

In acoustics, inclusions associated to Neumann boundary conditions correspond to sound hard inclusions, and the Helmholtz equation applies in two or three dimensions. In electromagnetism,

they correspond to metallic inclusions (perfectly conducting) in two dimensions, say invariant along the X_3-axis for waves for transverse magnetic waves (TM, the magnetic field H along $\mathbf{e}_3$). In this context, the magnetic field is a scalar function satisfying the Helmholtz equation, with Neumann boundary conditions on the metallic inclusions

$$\begin{cases} \Delta H + k^2 H = 0, \\ \boldsymbol{\nabla} H.\mathbf{n}_{|\partial\mathcal{D}} = 0, \end{cases} \tag{2.1}$$

with k the wavevector in the free space and the inclusions occupying $\mathcal{D}$. Note that this condition for a perfectly conducting metal has been regarded in detail when a thin structure is considered [35,36]. The field $\mathbf{H} = (0, 0, H)$ being known, the electric field $\mathbf{E} = (E_1, E_2, 0)$ can be deduced, if needed, with

$$\frac{\partial H}{\partial X_1} = \mathrm{i}\omega E_2, \quad \text{and} \quad \frac{\partial H}{\partial X_2} = -\mathrm{i}\omega E_1.$$

In this section, we shall establish that the periodic array of Neumann inclusions can be replaced by an equivalent interface across which jump conditions apply, Eqs. (2.16). Specifically, it will be shown that at the first order, the Neumann inclusions are transparent for the waves, Eqs. (2.10) and that their effects appear at the second order, Eqs. (2.14)-(2.15). Thus, in the equivalent homogenized problem, the field H and of its normal derivative are discontinuous across the interface.

(i) Asymptotic expansions and matching conditions

The natural small parameter is $\varepsilon = kh \ll 1$ and to be consistent, we need to write the Helmholtz equation in a dimensionless form, with $\mathbf{x} = k\mathbf{X}$ (and $H(\mathbf{x}) = H(\mathbf{X})$). Next, the problem is reformulated introducing the vector field $\boldsymbol{C} = \boldsymbol{\nabla}_{\mathbf{x}} H$

$$\begin{cases} \mathrm{div}_{\mathbf{x}} \boldsymbol{C} + H = 0, \quad \boldsymbol{C} \equiv \nabla_{\mathbf{x}} H, \\ \boldsymbol{C}.\mathbf{n}_{|\partial\mathcal{D}} = 0. \end{cases} \tag{2.2}$$

The solution can be expanded with respect to the small parameter ε, namely

$$\begin{aligned} H &= H^0(\mathbf{x}) + \varepsilon H^1(\mathbf{x}) + \varepsilon^2 H^2(\mathbf{x}) + \dots, \\ \boldsymbol{C} &= \boldsymbol{C}^0(\mathbf{x}) + \varepsilon \boldsymbol{C}^1(\mathbf{x}) + \varepsilon^2 \boldsymbol{C}^2(\mathbf{x}) + \dots \end{aligned} \tag{2.3}$$

In principle, this expansion can be used in the whole space (see *e.g.* [33]). Nevertheless, the resolution may be involved if the spatial derivatives in Eq. (2.2) make ε to appear. This is avoided using two ingredients: first, a separation of the space into an inner and an outer regions, which correspond to the near and far fields, respectively. In the outer region, the natural coordinates $\mathbf{x} \equiv (x_1, x_2, x_3)$ are adapted and the expansions, Eq. (2.3), apply. In the near field, as in the classical homogenization, a new system of coordinates $\mathbf{y} = \mathbf{x}/\varepsilon$ is introduced, able to account for the rapid variations of H, typically the variations with h (Fig. 2). Along x_2 and x_3, the wavefield satisfies pseudo periodic conditions associated to slow variations. This is accounted for by keeping $\mathbf{x}' \equiv (x_2, x_3)$ as additional coordinates. Accordingly, the expansions Eqs. (2.3) apply for the outer solution and, for the inner solution, we use the expansion

$$\begin{aligned} H &= h^0(\mathbf{y}, \mathbf{x}') + \varepsilon h^1(\mathbf{y}, \mathbf{x}') + \varepsilon^2 h^2(\mathbf{y}, \mathbf{x}') + \dots, \\ \boldsymbol{C} &= \mathbf{c}^0(\mathbf{y}, \mathbf{x}') + \varepsilon \mathbf{c}^1(\mathbf{y}, \mathbf{x}') + \varepsilon^2 \mathbf{c}^2(\mathbf{y}, \mathbf{x}') + \dots \end{aligned} \tag{2.4}$$

Finally, both regions are connected in some boundary region, where the evanescent field is vanishing at small x_1 values corresponding to $y_1 = x_1/\varepsilon \to \pm\infty$. These matching conditions are obtained using Taylor expansions for small x_1, $H^0(x_1, \mathbf{x}') = H^0(0, \mathbf{x}') + x_1 \partial_{x_1} H^0(0, \mathbf{x}') + \dots = H^0(0, \mathbf{x}') + \varepsilon y_1 \partial_{x_1} H^0(0, \mathbf{x}') + \dots$, same for $\boldsymbol{C}^0$, and identifying the terms in ε^n in the inner and outer expansions, Eqs. (2.3)-(2.4). We get, at the first and second orders

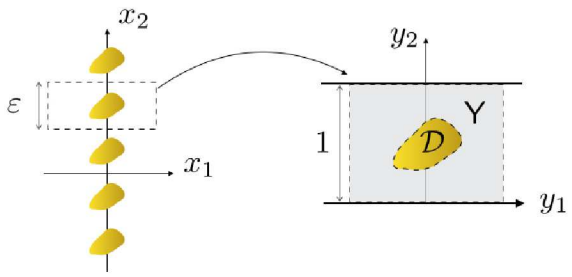

Figure 2. (a) Geometry of the array in non dimensional coordinates $\mathbf{x} = (x_1, x_2, x_3)$; (b) The inner problem in $\mathbf{y} = (y_1, y_2, y_3)$ coordinates; $\mathsf{Y} = [-y_1^m, y_1^m] \times [0,1]^2$; we define $\mathsf{Y}_\infty =]-\infty, \infty[\times[0,1]^2$ and $\mathbf{x}' = (x_2, x_3)$ and $\mathbf{y}' = (y_2, y_3)$.

$$H^0(0^\pm, \mathbf{x}') = \lim_{y_1 \to \pm\infty} h^0(\mathbf{y}, \mathbf{x}'), \tag{2.5a}$$

$$\boldsymbol{C}^0(0^\pm, \mathbf{x}') = \lim_{y_1 \to \pm\infty} \boldsymbol{c}^0(\mathbf{y}, \mathbf{x}'), \tag{2.5b}$$

$$H^1(0^\pm, \mathbf{x}') = \lim_{y_1 \to \pm\infty} \left[h^1(\mathbf{y}, \mathbf{x}') - y_1 \frac{\partial H^0}{\partial x_1}(0^\pm, \mathbf{x}') \right], \tag{2.6a}$$

$$\boldsymbol{C}^1(0^\pm, \mathbf{x}') = \lim_{y_1 \to \pm\infty} \left[\boldsymbol{c}^1(\mathbf{y}, \mathbf{x}') - y_1 \frac{\partial \boldsymbol{C}^0}{\partial x_1}(0^\pm, \mathbf{x}') \right], \tag{2.6b}$$

As in classical homogenization, the functions h^n and $\boldsymbol{c}^n$ are periodic with respect to $\mathbf{y}' \equiv (y_2, y_3)$. This is not meaningless in the present context if we have in mind the condition of pseudo periodicity. This condition is handled by the variable $\mathbf{x}'$, for instance $H^n(\mathbf{y}, x_2 + \varepsilon) = e^{ik_2 h} H^n(\mathbf{y}, x_2)$ in two dimensions, see Eqs. (2.5) and (2.6) for $n = 0, 1$ (the condition of pseudo periodicity applies for the outer solution $(H^n, \boldsymbol{C}^n)$). If one thinks to the H^n in terms of separable functions (and this will be the case) $H^n(\mathbf{y}, x_2) = f(\mathbf{y}) g(x_2)$, we recover the form of a Floquet solution, with $g(x_2) = e^{ik_2 x_2/k}$ and f periodic with respect to y_2.

(ii) Equations governing the inner and outer solutions - The elementary problems

The equations in the outer and inner problems can be written, from Eqs. (2.2), owing to

$$\begin{cases} \boldsymbol{\nabla} \to \boldsymbol{\nabla}_{\mathbf{x}}, & \text{in the outer problem,} \\ \boldsymbol{\nabla} \to \dfrac{1}{\varepsilon} \boldsymbol{\nabla}_{\mathbf{y}} + \boldsymbol{\nabla}_{\mathbf{x}'}, & \text{in the inner problem.} \end{cases}$$

(and we report only the equations that will be needed). We get for the outer problem

$$\mathrm{div}_{\mathbf{x}} \boldsymbol{C}^0 + H^0 = 0, \tag{2.7a}$$

$$\boldsymbol{C}^0 = \boldsymbol{\nabla}_{\mathbf{x}} H^0, \tag{2.7b}$$

and for the inner problem

$$\boldsymbol{\nabla}_{\mathbf{y}} h^0 = \mathbf{0}, \tag{2.8a}$$

$$\mathrm{div}_{\mathbf{y}} \boldsymbol{c}^0 = 0, \tag{2.8b}$$

$$\boldsymbol{c}^0 = \boldsymbol{\nabla}_{\mathbf{y}} h^1 + \boldsymbol{\nabla}_{\mathbf{x}'} h^0, \tag{2.8c}$$

$$\mathrm{div}_{\mathbf{y}} \boldsymbol{c}^1 + \mathrm{div}_{\mathbf{x}'} \boldsymbol{c}^0 + h^0 = 0. \tag{2.8d}$$

The boundary conditions on the Neumann inclusions apply in the inner problem, namely

$$\boldsymbol{c}^0.\mathbf{n}_{|\partial\mathcal{D}} = \boldsymbol{c}^1.\mathbf{n}_{|\partial\mathcal{D}} = 0, \tag{2.9}$$

while the boundary conditions for the outer problem are given by the matching conditions.

First, we shall show that the inclusions are not seen at the first order. The Eq. (2.8*a*) shows that h^0 does not depend on $\mathbf{y}$ and Eq. (2.8*b*) shows that $\int \mathrm{d}\mathbf{y}'\, c_1^0(-\infty, \mathbf{y}', \mathbf{x}') = \int \mathrm{d}\mathbf{y}'\, c_1^0(+\infty, \mathbf{y}', \mathbf{x}')$. This latter relation is obtained by integrating $\mathrm{div}_{\mathbf{y}} \boldsymbol{c}^0 = 0$ over $\mathsf{Y}_\infty \backslash \mathcal{D}$ (with $\mathsf{Y}_\infty =]-\infty, +\infty[\times[0,1]^2$) using the boundary condition, Eq. (2.9), and owing to the periodicity of $\boldsymbol{c}^0$ with respect to $\mathbf{y}'$. From Eqs (2.5), we get $H^0(0^\pm, \mathbf{x}') = h^0(\mathbf{x}')$, and $C_1^0(0^\pm, \mathbf{x}') = \int \mathrm{d}y_2\, c_1^0(\pm\infty, \mathbf{y}', \mathbf{x}')$, whence the jump conditions at the first order read

$$\left[\!\left[H^0 \right]\!\right] = \left[\!\left[C_1^0 \right]\!\right] = 0. \tag{2.10}$$

The inclusions are transparent at the first order, with H^0 and $\boldsymbol{C}^0$ being continuous across the equivalent interface. To capture the effect of the Neumann inclusions, we need to go at the second order. This second order involves h^1 and $\boldsymbol{c}^0$ and it is easy to see that h^1 satisfies

$$\begin{cases} \mathrm{div}_{\mathbf{y}} \left[\boldsymbol{\nabla}_{\mathbf{y}} h^1 + \boldsymbol{\nabla}_{\mathbf{x}'} H^0(0, \mathbf{x}') \right] = 0, \\ \left[\boldsymbol{\nabla}_{\mathbf{y}} h^1 + \boldsymbol{\nabla}_{\mathbf{x}'} H^0(0, \mathbf{x}') \right] .\mathbf{n}_{|\partial\mathcal{D}} = 0, \\ \lim\limits_{y_1 \to \pm\infty} \boldsymbol{\nabla}_{\mathbf{y}} h^1 = \dfrac{\partial H^0}{\partial x_1}(0, \mathbf{x}') \mathbf{e}_1. \end{cases} \tag{2.11}$$

The first equation in the above system comes from Eqs. (2.8*b*)-(2.8*c*), using $H^0(0, \mathbf{x}') = h^0(\mathbf{x}')$. The second equation corresponds to the boundary condition, Eq. (2.9) with $c^0 = \boldsymbol{\nabla}_{\mathbf{y}} h^1 + \boldsymbol{\nabla}_{\mathbf{x}'} H^0(0, \mathbf{x}')$, from (2.8*c*) with $h^0(\mathbf{x}) = H^0(0, \mathbf{x}')$. The third equation corresponds to the matching conditions Eq. (2.5*b*), with $\boldsymbol{C}^0 = \partial_{x_1} H^0 \mathbf{e_1} + \boldsymbol{\nabla}_{\mathbf{x}'} H^0$, and $\boldsymbol{C}^0$ being continuous. By linearity of the above system, the problem can be divided into elementary problems being independent of $\mathbf{x}'$. Specifically, h^1 can be written

$$h^1(\mathbf{y}, \mathbf{x}') = \frac{\partial H^0}{\partial x_1}(0, \mathbf{x}') \left[h^{(1)}(\mathbf{y}) + y_1 \right] + \frac{\partial H^0}{\partial x_\alpha}(0, \mathbf{x}') h^{(\alpha)}(\mathbf{y}) + \tilde{h}(\mathbf{x}'), \tag{2.12}$$

with $\alpha = 2, 3$ and where the functions $h^{(i)}(\mathbf{y})$, $i = 1, 2, 3$, satisfy the

$$\text{elementary problems:} \begin{cases} \Delta h^{(i)} = 0, \\ \boldsymbol{\nabla} h^{(i)} .\mathbf{n}_{|\partial\mathcal{D}} = -\mathbf{e}_i .\mathbf{n}_{|\partial\mathcal{D}} \\ \lim\limits_{y_1 \to \pm\infty} \boldsymbol{\nabla} h^{(i)} = \mathbf{0}. \end{cases} \tag{2.13}$$

The field h^1 in Eqs. (2.11) is defined up to the function $\tilde{h}(\mathbf{x}')$, but we will see that the equivalent conditions do not require $\tilde{h}$ to be determined in Eq. (2.12).

(iii) The interface parameters and the jump conditions at the equivalent zero thickness interface

In this section, we derive the jump conditions appearing at the second order in ε. These jump conditions involve interface parameters coming from the elementary problems that we have defined in Eqs. (2.13).

First, the effective condition on H^1 is obtained using the matching condition Eq. (2.6*a*) (with $\partial_{x_i} H^0$ continuous at $x_1 = 0$) and the Eq. (2.12). We get

$$H^1(0^{\pm}, \mathbf{x}') = \frac{\partial H^0}{\partial x_i}(0, \mathbf{x}') h^{(i)}(\pm\infty, \mathbf{y}').$$

from which the jump condition on H^1 is deduced

$$\left[\!\left[H^1 \right]\!\right] = \frac{\partial H^0}{\partial x_i}(0, \mathbf{x}') \left(h^{(i)}(+\infty, \mathbf{y}') - h^{(i)}(-\infty, \mathbf{y}') \right). \tag{2.14}$$

Next, we want the jump condition on $\boldsymbol{C}^1$. To that aim, we need the expression of $\boldsymbol{c}^0$ and, from Eqs. (2.7*a*)-(2.7*b*), (2.8*c*) and (2.12), we get

$$\boldsymbol{c}^0(\mathbf{y}, \mathbf{x}') = \boldsymbol{C}^0(0, \mathbf{x}') + C_i^0(0, \mathbf{x}') \boldsymbol{\nabla}_{\mathbf{y}} h^{(i)}(\mathbf{y}).$$

Now, Eq. (2.8*d*) reads

$$\mathrm{div}_{\mathbf{y}} \boldsymbol{c}^1(\mathbf{y}, \mathbf{x}') + \frac{\partial C_i^0}{\partial x_\alpha}(0, \mathbf{x}') \frac{\partial h^{(i)}}{\partial y_\alpha}(\mathbf{y}) - \frac{\partial C_1^0}{\partial x_1}(0, \mathbf{x}') = 0.$$

Integrating the above relation over $\mathsf{Y} \backslash \mathcal{D}$ and owing to the periodicity of $\boldsymbol{c}^1$ with respect to $\mathbf{y}'$, we get

$$\int \mathrm{d}\mathbf{y}' \left[c_1^1(y_1^m, \mathbf{y}', \mathbf{x}') - c_1^1(-y_1^m, \mathbf{y}', \mathbf{x}') \right] - \frac{\partial C_1^0}{\partial x_1}(0, \mathbf{x}') \left(2y_1^m - \mathcal{S} \right) + \frac{\partial C_i^0}{\partial x_\alpha} \int_{\mathsf{Y} \backslash \mathcal{D}} \mathrm{d}\mathbf{y} \frac{\partial h^{(i)}}{\partial y_\alpha}(\mathbf{y}) = 0,$$

with $\alpha = 2, 3$ and where $\mathcal{S}$ is the surface of $\mathcal{D}$ in the $\mathbf{y}$ coordinates. Taking the limit $y_1^m \to +\infty$ and using Eq. (2.6*b*), we get

$$\left[\!\left[C_1^1 \right]\!\right] = -\frac{\partial C_1^0}{\partial x_1}(0, \mathbf{x}') \, \mathcal{S} - \frac{\partial C_i^0}{\partial x_\alpha}(0, \mathbf{x}') \int_{\mathsf{Y}_\infty \backslash \mathcal{D}} \mathrm{d}\mathbf{y} \frac{\partial h^{(i)}}{\partial y_\alpha}. \tag{2.15}$$

It is now sufficient to remark that $[\![H]\!] = \varepsilon \left[\!\left[H^1 \right]\!\right] + O(\varepsilon^2)$ and $\partial_{x_1} H = \partial_{x_1} H^0 + O(\varepsilon)$ (and the same for $\boldsymbol{C}$) to get the jump conditions in the real space, equivalent to Eqs. (2.14)-(2.15) up to $O(\varepsilon^2)$

$$\text{Jump conditions} \begin{cases} [\![H]\!] = h \, \mathcal{B}_i \, \dfrac{\partial \bar{H}}{\partial X_i}(0, \mathbf{X}'), \\ \left[\!\left[\dfrac{\partial H}{\partial X_1} \right]\!\right] = -h \, \mathsf{C}_{ij} \, \dfrac{\partial^2 \bar{H}}{\partial X_i \partial X_j}(0, \mathbf{X}'). \end{cases} \tag{2.16}$$

with

$$\begin{cases} \mathcal{B}_i = h^{(i)}(+\infty, \mathbf{y}') - h^{(i)}(-\infty, \mathbf{y}'), \\ \mathsf{C}_{11} = S, & \mathsf{C}_{1\alpha} = \displaystyle\int_{\mathsf{Y}_\infty \backslash \mathcal{D}} \mathrm{d}\mathbf{y} \frac{\partial h^{(1)}}{\partial y_\alpha}, \\ \mathsf{C}_{\alpha 1} = 0, & \mathsf{C}_{\alpha\beta} = \displaystyle\int_{\mathsf{Y}_\infty \backslash \mathcal{D}} \mathrm{d}\mathbf{y} \frac{\partial h^{(\alpha)}}{\partial y_\beta}. \end{cases} \tag{2.17}$$

It is essential that the elementary problems, Eqs. (2.13), do not depend on the incident wave (as the former problem Eqs. (2.11) does, through H^0). This ensures that the parameters in Eqs. (2.17) are characteristic of the interface independently of the scattering problem considered. Incidentally, this also means that the elementary problems will be solved once and for all.

The obtained jump conditions for H and its normal derivative involve 9 interface parameters in three dimensions, one of which being the surface of inclusion; in two dimensions, only 5 parameters are needed. Next, for inclusion shapes being symmetric with respect to $\mathbf{y}'$, $h^{(1)}$ is symmetric *w.r.t.* $\mathbf{y}'$, from which $\mathsf{C}_{1\alpha} = \int_{Y\setminus\mathcal{D}} \mathrm{d}\mathbf{y}\, \partial_{y_\alpha} h^{(1)} = 0$. Then, $h^{(\alpha)}$ ($\alpha = 2, 3$) being antisymmetric *w.r.t.* $\mathbf{y}'$ in this case, we also have $\mathcal{B}_i = 0$ ($h^{(\alpha)}(+\infty, 0, 0) = h^{(\alpha)}(-\infty, 0, 0) = 0$); it follows that only 5 interface parameters in three dimensions and 3 interface parameters in two dimensions are needed for symmetrical inclusions.

(b) Inclusions associated to Dirichlet boundary conditions

In the context of electromagnetism, Dirichlet boundary conditions apply for a perfect conductor in transverse electric polarization (TE), which means that $\mathbf{E} = (0, 0, E)$ is transverse, and $\mathbf{H} = (H_1, H_2, 0)$ is an in-plane vector. The Helmholtz equation applies for the scalar electric field E

$$\begin{cases} \Delta E + k^2 E = 0, \\ E_{|\partial\mathcal{D}} = 0, \end{cases} \tag{2.18}$$

afterwards $H_1 = -\mathrm{i}/\omega\, \partial E/\partial X_2$ and $H_2 = \mathrm{i}/\omega\, \partial E/\partial X_1$ can be deduced if they are needed.

In this section, we shall use the same approach as in the previous one, but the result for an array of Dirichlet inclusions significantly differ from the Neumann case. Indeed, we shall obtain boundary conditions at an equivalent, homogenized, flat surface instead of the jump conditions obtained for Neumann inclusions. These boundary conditions tell us that, at the first order, the array of Dirichlet inclusions is equivalent to a surface entirely associated to Dirichlet boundary condition (see Eq. (2.24)). Thus, imposing a vanishing electric field at periodic places along a surface is sufficient to cancel (at dominant order) the field over the whole surface. In the context of holes in elasticity, this has been entitled 'the principle of the dressmaker' [21], that is to say, 'it is not necessary to sew entirely two pieces of fabrics in order to render invisible their relative opening, it is sufficient to sew them at a great number of points regularly spaced'.

At the dominant order, the inclusions are thus visible but not their structuration and this latter is captured at the second order only, leading to the final boundary conditions Eqs. (2.31).

As in Sec. 2.(a), we start by reformulating (2.18) in the rescaled space $\mathbf{x} = k\mathbf{X}$, with $E(\mathbf{x}) = E(\mathbf{X})$

$$\begin{cases} \mathrm{div}_{\mathbf{x}} \boldsymbol{G} + E = 0, \quad \boldsymbol{G} \equiv \nabla_{\mathbf{x}} E, \\ E_{|\partial\mathcal{D}} = 0. \end{cases} \tag{2.19}$$

The expansions are then the same as in the TM case, with

$$\begin{aligned} \text{Outer exp.} & \begin{cases} E = E^0(\mathbf{x}) + \varepsilon E^1(\mathbf{x}) + \varepsilon^2 E^2(\mathbf{x}) + \dots, \\ \boldsymbol{G} = \boldsymbol{G}^0(\mathbf{x}) + \varepsilon \boldsymbol{G}^1(\mathbf{x}) + \varepsilon^2 \boldsymbol{G}^2(\mathbf{x}) + \dots \end{cases} \\ \text{Inner exp.} & \begin{cases} E = e^0(\mathbf{y}, \mathbf{x}') + \varepsilon e^1(\mathbf{y}, \mathbf{x}') + \varepsilon^2 e^2(\mathbf{y}, \mathbf{x}') + \dots, \\ \boldsymbol{G} = \boldsymbol{g}^0(\mathbf{y}, \mathbf{x}') + \varepsilon \boldsymbol{g}^1(\mathbf{y}, \mathbf{x}') + \varepsilon^2 \boldsymbol{g}^2(\mathbf{y}, \mathbf{x}') + \dots \end{cases} \end{aligned} \tag{2.20}$$

and the matching conditions read, at the first order

$$E^0(0^{\pm},\mathbf{x}') = \lim_{y_1\to\pm\infty} e^0(\mathbf{y},\mathbf{x}'), \tag{2.21a}$$

$$\boldsymbol{G}^0(0^{\pm},\mathbf{x}') = \lim_{y_1\to\pm\infty} \boldsymbol{g}^0(\mathbf{y},\mathbf{x}'), \tag{2.21b}$$

and at the second order

$$E^1(0^{\pm},\mathbf{x}') = \lim_{y_1\to\pm\infty} \left[e^1(\mathbf{y},\mathbf{x}') - y_1 \frac{\partial E^0}{\partial x_1}(0^{\pm},\mathbf{x}') \right], \tag{2.22}$$

(the matching condition on $\boldsymbol{G}^1$ is not needed). The equations in the inner and outer problems are the same as in Eqs. (2.7)-(2.8) owing to $B^n \to E^n$, $\boldsymbol{C}^n \to \boldsymbol{G}^n$ (and $b^n \to e^n$, $\boldsymbol{c}^n \to \boldsymbol{g}^n$), while boundary conditions in the inner problem now read

$$e^0_{|\partial\mathcal{D}} = e^1_{|\partial\mathcal{D}} = 0. \tag{2.23}$$

At the first order, $\boldsymbol{\nabla}_{\mathbf{y}} e^0 = 0$ and this tells us that e^0 does not depend on $\mathbf{y}$. Next, we have $e^0_{|\partial\mathcal{D}} = 0$; because this boundary condition is expressed in terms of the spatial coordinate $\mathbf{y}$, and that e^0 does not depend on $\mathbf{y}$, we conclude that $e^0 = 0$ everywhere. It follows that

$$e^0 = E^0(0,\mathbf{x}') = 0, \quad \text{and} \quad \frac{\partial E^0}{\partial x_\alpha}(0,\mathbf{x}') = 0, \tag{2.24}$$

with $\alpha = 2, 3$ (the second equation is simply a consequence of the first one). At the first order, we find $E^0(0,\mathbf{x}') = 0$ which means that the Dirichlet inclusions are visible, and they are equivalent to a flat surface associated to Dirichlet boundary conditions. Nevertheless, their structuration in array is not visible and to capture this structuration effect, we need to go up to the second order.

To go up to the second order, we start with the outer problem. With $\boldsymbol{G}^0 = \boldsymbol{\nabla}_{\mathbf{x}} E^0$, and using $\partial_{x_\alpha} E^0(0,\mathbf{x}') = 0$ from (2.24), we get

$$\boldsymbol{G}^0(0^{\pm},\mathbf{x}') = \frac{\partial E^0}{\partial x_1}(0^{\pm},\mathbf{x}')\mathbf{e}_1, \tag{2.25}$$

and $\boldsymbol{G}^0$ is not continuous *a priori* at $x_1 = 0$. Now, the goal is to determine $E^1(0^{\pm}, x_2)$. In the inner problem, Eqs. (2.8*b*) and (2.8*c*) read $\mathrm{div}_{\mathbf{y}} \boldsymbol{g}^0 = 0$ and $\boldsymbol{g}^0 = \boldsymbol{\nabla}_{\mathbf{y}} e^1 + \boldsymbol{\nabla}_{\mathbf{x}'} e^0$. As e^0 is constant, the latter equation simplifies in $\boldsymbol{g}^0 = \boldsymbol{\nabla}_{\mathbf{y}} e^1$. It follows that e^1 satisfies the Laplace equation associated to Dirichlet boundary condition on $\partial\mathcal{D}$; finally, accounting for the matching condition Eq. (2.21*b*), with Eq. (2.25), e^1 satisfies

$$\begin{cases} \Delta e^1 = 0, \\ \lim\limits_{y_1\to\pm\infty} \boldsymbol{\nabla}_{\mathbf{y}} e^1 = \dfrac{\partial E^0}{\partial x_1}(0^{\pm},\mathbf{x}')\mathbf{e}_1, \\ e^1_{|\partial\mathcal{D}} = 0. \end{cases} \tag{2.26}$$

Owing to the linearity of the above system, we can write

$$e^1(\mathbf{y},x_2) = \frac{\partial E^0}{\partial x_1}(0^+,\mathbf{x}')e^{(+)}(\mathbf{y}) + \frac{\partial E^0}{\partial x_1}(0^-,\mathbf{x}')e^{(-)}(\mathbf{y}), \tag{2.27}$$

with $e^{(\pm)}$ solutions of the elementary problems:

$$\begin{cases} \Delta_{\mathbf{y}} e^{(\pm)} = 0, \\ \lim\limits_{y_1 \to -\infty} \boldsymbol{\nabla}_{\mathbf{y}} e^{(+)} = \mathbf{0}, \quad \lim\limits_{y_1 \to +\infty} \boldsymbol{\nabla}_{\mathbf{y}} e^{(+)} = \mathbf{e}_1, \\ \lim\limits_{y_1 \to -\infty} \boldsymbol{\nabla}_{\mathbf{y}} e^{(-)} = \mathbf{e}_1, \quad \lim\limits_{y_1 \to +\infty} \boldsymbol{\nabla}_{\mathbf{y}} e^{(-)} = \mathbf{0}, \\ e^{(\pm)}_{|\partial\mathcal{D}} = 0. \end{cases} \tag{2.28}$$

These elementary problems correspond to the electrostatic problems of an infinite periodic row of line charges, with a unitary electric field being imposed at $y_1 \to -\infty$ (potential $e^{(-)}$) or imposed at $y_1 \to +\infty$ (potential $e^{(+)}$). This problem has been revisited recently in the context of the Faraday cage problem [37]. The general solution $e^{(+)}$ is of the form

$$\begin{cases} e^{(+)}(y_1 < 0) = \mathcal{C}_1^+ + e_{\text{ev}}^+, \\ e^{(+)}(y_1 > 0) = y_1 + \mathcal{C}_2^+ + e_{\text{ev}}^+, \end{cases} \tag{2.29}$$

and

$$\begin{cases} e^{(-)}(y_1 < 0) = y_1 + \mathcal{C}_2^- + e_{\text{ev}}^-, \\ e^{(-)}(y_1 > 0) = \mathcal{C}_1^- + e_{\text{ev}}^-, \end{cases} \tag{2.30}$$

with $e_{\text{ev}}^{\pm}$ are evanescent fields vanishing at $y_1 \to \pm\infty$. Integrating $e^{(+)}\Delta e^{(-)} = 0$ and $e^{(-)}\Delta e^{(+)} = 0$ over $\mathsf{Y}_\infty \backslash \mathcal{D}$, it is easy to see that $\int \mathrm{d}\mathbf{y}\, \boldsymbol{\nabla} e^{(+)} \boldsymbol{\nabla} e^{(-)} = \mathcal{C}_1^- = -\mathcal{C}_1^+$ and we denote $\mathcal{C}_1 = \mathcal{C}_1^+$.

It is now sufficient to use the matching condition, Eq. (2.22), and coming back to the real space $E(\mathbf{x}) = E(\mathbf{X})$, we get the equivalent boundary condition at the zero thickness interface

$$\begin{cases} E(0^+, \mathbf{X}') = h\mathcal{C}_2^+ \dfrac{\partial E}{\partial X_1}(0^+, \mathbf{X}') - h\mathcal{C}_1 \dfrac{\partial E}{\partial X_1}(0^-, \mathbf{X}'), \\ E(0^-, \mathbf{X}') = h\mathcal{C}_1 \dfrac{\partial E}{\partial X_1}(0^+, \mathbf{X}') + h\mathcal{C}_2^- \dfrac{\partial E}{\partial X_1}(0^-, \mathbf{X}'), \end{cases} \tag{2.31}$$

where we have used $E = \varepsilon E^1 + O(\varepsilon^2)$ and $\partial E/\partial x_1 = \partial E^0/\partial x_1 + O(\varepsilon)$. The boundary conditions involve 3 interface parameters both in 2D and 3D. For inclusions being symmetrical with respect to y_1, $e^{(-)}(y_1) = -e^{(+)}(-y_1)$ from which $\mathcal{C}_2^- = -\mathcal{C}_2^+$, leading to 2 interface parameters.

3. Validation of the effective interface conditions for 2D rectangular inclusions

We inspect the validity of our model for a plane wave at oblique incidence on an array of rectangular metallic inclusions (Fig. 3). Once the interface parameters have been calculated, the jump conditions in TM, Eqs. (2.16), or the boundary conditions in TE, Eqs. (2.31), can be applied leading to explicit expression of the solution. We compare our solutions with the solutions obtained with full wave calculations and we discuss the range of validity of the interface homogenization in terms of the small parameters ke and kh.

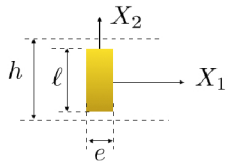

Figure 3. Unit cell of the array of rectangular inclusion in the 2D problem.

(a) The case of transverse magnetic polarization

(i) The interface parameters for 2D rectangular inclusions

In 2 dimensions, the elementary problems, for $i=1,2$, have to been solved, Eqs. (2.13), which makes in general 5 interface parameters to determine $(\mathcal{B}_1,\mathcal{B}_2,\mathcal{C}_{11}=\mathcal{S},\mathcal{C}_{12},\mathcal{C}_{22})$; as previously said, for symmetric inclusions, only 3 do not vanish, and we note $\mathcal{B}\equiv\mathcal{B}_1$ and $\mathcal{C}\equiv \mathsf{C}_{22}$. These parameters are

$$\left\{\begin{array}{l} \mathcal{S}=e\ell, \\ \mathcal{B}=\dfrac{e\ell}{h(h-\ell)}+\mathcal{B}_0, \quad \text{with } \mathcal{B}_0\equiv\dfrac{2}{\pi}\log\left(\sin\pi\dfrac{(h-\ell)}{2h}\right)^{-1}, \\ \mathcal{C}=\displaystyle\int_0^1 \mathrm{d}y\,\frac{\partial h^{(2)}}{\partial y_2}, \text{ with } h^{(2)} \text{ solution of } \quad \Delta h^{(2)}=0, \quad \boldsymbol{\nabla}\left(h^{(2)}+y_2\right).\mathbf{n}_{|\partial\mathcal{D}}=0, \quad \lim_{y_1\to\pm\infty}\boldsymbol{\nabla}h^{(2)}=\mathbf{0}. \end{array}\right. \tag{3.1}$$

and they are involved in the jump conditions, Eqs. (2.16), which simplify to

$$\left\{\begin{array}{l} [\![H]\!]=h\mathcal{B}\,\dfrac{\partial\bar{H}}{\partial X_1}(0,\mathbf{X}'), \\ \left[\!\!\left[\dfrac{\partial H}{\partial X_1}\right]\!\!\right]=-h\mathcal{S}\,\dfrac{\partial^2\bar{H}}{\partial X_1^2}(0,\mathbf{X}')-h\mathcal{C}\,\dfrac{\partial^2\bar{H}}{\partial X_2^2}(0,\mathbf{X}'). \end{array}\right. \tag{3.2}$$

The surface of the inclusion $\mathcal{S}$ is always known, here $\mathcal{S}=e\ell$. For rectangular inclusions, the derivation of the so-called blockage coefficient $\mathcal{B}$ can be found in [38]. For flat plate ($e=0$), $\mathcal{B}=\mathcal{B}_0$ has been derived independently in acoustics [39] and in electromagnetism [40]. To our knowledge, no such explicit expression exists for $\mathcal{C}$, which has been solved numerically using mode matching technique (typical behaviors of these parameters are reported in Figs. 10).

(ii) Validation for the scattering of an incident plane wave

Here, we consider a simple scattering problem, with an incident plane wave at incidence θ

$$\left\{\begin{array}{l} H(X_1>0,X_2)=e^{\mathrm{i}k\sin\theta X_2}\left[e^{\mathrm{i}k\cos\theta X_1}+Re^{-\mathrm{i}k\cos\theta X_1}\right], \\ H(X_1<0,X_2)=e^{\mathrm{i}k\sin\theta X_2}\,Te^{\mathrm{i}k\cos\theta X_1}. \end{array}\right. \tag{3.3}$$

Applying the boundary conditions, Eqs. (3.2), to Eq. (3.3), we find

$$\left\{\begin{array}{l} R=-\mathrm{i}\,\dfrac{a+b}{(1+\mathrm{i}a)(1-\mathrm{i}b)}, \quad T=\dfrac{1-ab}{(1+\mathrm{i}a)(1-\mathrm{i}b)}, \\ \text{with } a\equiv\dfrac{kh}{2}\cos\theta\,\left(\mathcal{S}+\mathcal{C}\tan^2\theta\right),\ b\equiv\dfrac{kh}{2}\cos\theta\,\mathcal{B}. \end{array}\right. \tag{3.4}$$

(and because all fields are discontinuous at $X_1=0$, we used the definition in (1.1)).

The Figs. 4 and 5 illustrate the validity of the interface model. In Fig. 4, the H-field is calculated using full wave numerics and compared to the field given by Eqs. (3.3) with Eqs. (3.4); in the presented case, with $e/h=0.1$ and $\ell/h=0.95$, the interface parameters are $\mathcal{S}=0.095$, $\mathcal{B}=3.52$ and $\mathcal{C}=-0.004$. The fields are found to be in good agreement (5% discrepancy) although we have chosen a relatively high frequency $kh=1$.

In Fig. 5, we reported the reflection coefficient calculated using full wave numerics ($|R^{ex}|$, blue lines) and the reflection coefficient given by Eq. (3.4) ($|R|$, black dotted lines) as a function of e/h for $kh=1$ and $kh=0.1$. It is noticeable that $|R|$ does not vanish for $e/h\to 0$; this is expected since an array of flat inclusions ($e=0$), or strips, are able to scatter a wave, and this is attributable to the parameter $\mathcal{B}=\mathcal{B}_0$ which does not vanish for vanishing inclusion thickness.

Inspecting higher values of kh would reveal that our prediction fails for $kh>1$, as expected within homogenization theories. Next, from Fig. 5, it appears that the model is valid for $ke<1$ and $kh<1$; this is not very surprising and it confirms that the wavelength is the natural scale to discriminate between thin and thick films.

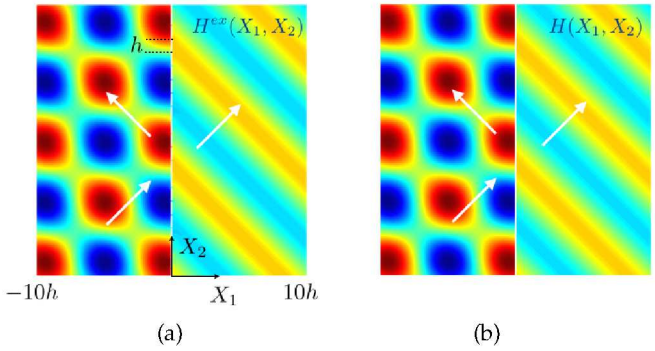

Figure 4. Wavefields in the (X_1, X_2) plane for $kh = 1$ with rectangular inclusions $e/h = 0.1$ and $\ell/h = 0.95$. (a) $H^{ex}(\mathbf{X})$ calculated numerically and (b) $H(\mathbf{X})$ coming from the homogenized interface model, Eq. (3.3), with Eqs. (3.4). The interface parameters are $\mathcal{S} = 0.095$, $\mathcal{B} = 3.52$ and $\mathcal{C} = -0.004$.

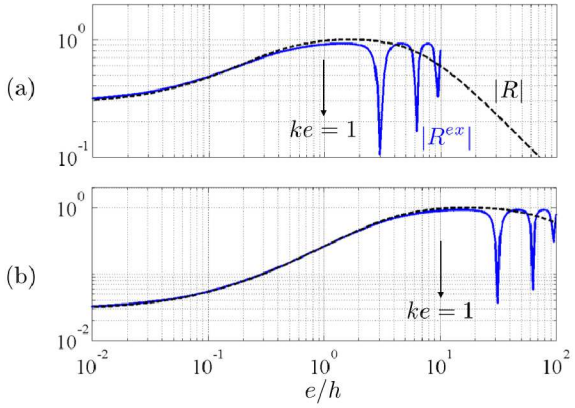

Figure 5. Variations of the reflection coefficients $|R^{ex}|$ calculated numerically (blue lines), and of $|R|$ given by the homogenized interface model, Eq. (3.4) (black dotted lines) as a function of e/h for (a) $kh = 1$ and (b) $kh = 10^{-1}$. Otherwise, $\ell = 0.9h$ and $\theta = \pi/3$.

(b) The case of transverse electric polarization

Rectangular inclusions being symmetric, only 2 interface parameters have to be determined, ($\mathcal{C}_1 = \mathcal{C}_1^+ = -\mathcal{C}_1, \mathcal{C}_2 = \mathcal{C}_2^+ = -\mathcal{C}_2^-$) in the elementary problem Eqs. (2.28)-(2.29), namely

$$\left\{\begin{array}{l} \mathcal{C}_1 = \lim\limits_{y_1\to+\infty}\left(e^{(+)} - y_1\right), \quad \mathcal{C}_2 = \lim\limits_{y_1\to-\infty} e^{(+)} \\ \text{with } e^{(+)}(y_1,y_2) \text{ solution of: } \Delta e^{(+)} = 0, \quad e^{(+)}_{|\partial\mathcal{D}} = 0, \quad \lim\limits_{y_1\to-\infty}\boldsymbol{\nabla} e^{(+)} = \mathbf{0}, \quad \lim\limits_{y_1\to+\infty}\boldsymbol{\nabla} e^{(+)} = \mathbf{e}_1. \end{array}\right. \tag{3.5}$$

For $e \neq 0$, explicit expressions of $(\mathcal{C}_1, \mathcal{C}_2)$ defined in the elementary problems Eqs. (2.28)-(2.29) are not available in the literature and they have been calculated solving numerically the elementary problem for $e^{(+)}$, Eqs. (2.28)-(2.29), see Figs. 11. However, an explicit expression for $e = 0$ is available [13,40], see Section 4.(a); in this case

$$\text{for } e = 0, \quad \mathcal{C}_1 = \mathcal{C}_2 = \frac{2}{\pi}\log\left(\sin\pi\frac{\ell}{2h}\right)^{-1}. \tag{3.6}$$

Thus, we get simplified effective boundary conditions, from Eqs. (2.31),

$$\left\{\begin{array}{l} E(0^+,\mathbf{X}') = h\mathcal{C}_2\dfrac{\partial E}{\partial X_1}(0^+,\mathbf{X}') - h\mathcal{C}_1\dfrac{\partial E}{\partial X_1}(0^-,\mathbf{X}'), \\ E(0^-,\mathbf{X}') = h\mathcal{C}_1\dfrac{\partial E}{\partial X_1}(0^+,\mathbf{X}') - h\mathcal{C}_2\dfrac{\partial E}{\partial X_1}(0^-,\mathbf{X}'). \end{array}\right. \tag{3.7}$$

As for the TM case, we consider the simple scattering problem of an incident plane wave at oblique incidence θ, for which the solution takes the form

$$\left\{\begin{array}{l} E(X_1>0,X_2) = e^{\mathrm{i}k\sin\theta X_2}\left[e^{\mathrm{i}k\cos\theta X_1} + Re^{-\mathrm{i}\cos\theta X_1}\right], \\ E(X_1<0,X_2) = e^{\mathrm{i}k\sin\theta X_2}\, Te^{\mathrm{i}\cos\theta X_1}. \end{array}\right. \tag{3.8}$$

Applying the boundary conditions Eqs. (3.7), we get (R,T)

$$\left\{\begin{array}{l} R = -\dfrac{1+c_2^2-c_1^2}{1+c_1^2-c_2^2-2\mathrm{i}c_2}, \quad T = -\dfrac{2\mathrm{i}c_1}{1+c_1^2-c_2^2-2\mathrm{i}c_2}, \\ \text{with } c_1 \equiv kh\cos\theta\,\mathcal{C}_1,\ c_2 \equiv kh\cos\theta\,\mathcal{C}_2. \end{array}\right. \tag{3.9}$$

Figs. 6 show the electric field E^{ex} calculated in full wave numerics compared to the field E in the homogenized problem, Eqs. (3.8)-(3.9). In the presented case $e/h=0.1$, $\ell/h=0.05$ (leading to $\mathcal{C}_1=0.209$, $\mathcal{C}_2=0.201$) and $kh=1$, and we have $|E-E^{ex}|/|E^{ex}|\simeq 6\%$ (the agreement becomes better for smaller kh value).

Next, in Figs. 7, we report the variations of $|R^{ex}+1|$ as a function of e/h for $kh=1$ and $kh=10^{-1}$ (with $|R|\simeq 1$ in the whole range of e/h, the variations of R are essentially encapsulated in its phase, which is regarded here in $|R+1|$ as the shift to a phase equal π). The conclusion is the same as in the TM case, namely that the interface homogenization is valid for $ke<1$ (note that, in this case, no result exists in classical homogenization).

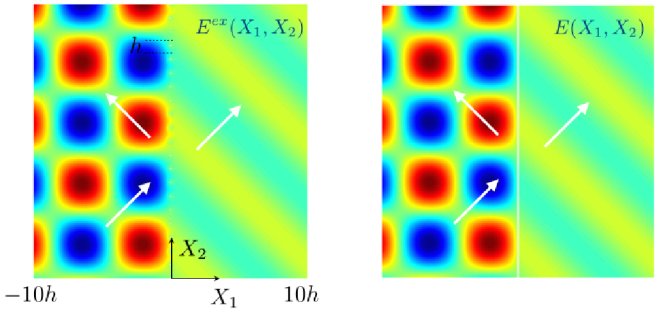

Figure 6. Wavefields in the (X_1,X_2) plane for $kh=1$ with rectangular inclusions $e/h=0.1$ and $\ell/h=0.95$. (a) $E^{ex}(\mathbf{X})$ calculated numerically and (b) $E(\mathbf{X})$ coming from the homogenized interface model, Eq. (3.8), with Eqs. (3.9). The interface parameters are $\mathcal{C}_1=0.209, \mathcal{C}_2=0.201$.

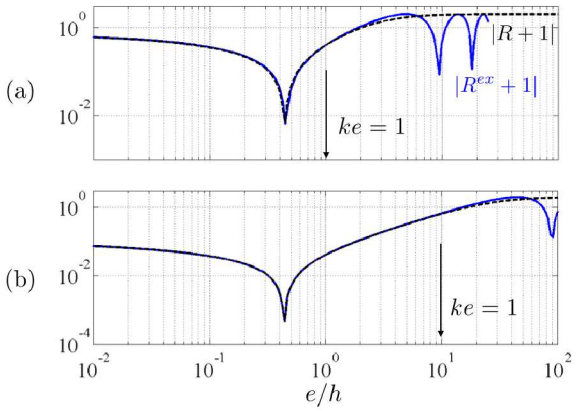

Figure 7. Variations of the reflection coefficients $|R^{ex}+1|$ calculated numerically (blue lines) and of $|R+1|$ given by the homogenized interface model, Eq. (3.4) (black dotted lines) as a function of e/h for $kh=1$ and 10^{-1}. Otherwise, $\ell=0.9h$ and $\theta=\pi/3$.

4. Comparison with existing models

(a) Comparison with the impedance surface theory

The transmission line theory is the most classical model to deal with devices composed of metallic screens and dielectric slabs. For the metallic parts, it is based on the relations voltage/electric field and current/magnetic field which can be written explicitly in some simplified cases (typically parallel plates), and which lead to the notion of effective impedances calculated in the quasi-static limit (and in general for particular polarizations of the wave, TM or TE). As soon as the effective impedances of each component of a device are known, an equivalent circuit can be explicitly built, from which boundary conditions are obtained. Probably the most important limitation of this model is that it it is restricted to specific geometries of the metallic screens in order to recognize inductances and capacitances. Also, explicit expressions being obtained for a host medium being identical on both sides of the metallic screen, the case of two different host media are deduced heuristically, using averaged permittivity.

Here, we inspect the simple cases of capacitive and inductive strips in free space, Fig. 8 (more involved geometries can be found in [13,14]). Following [14], the array of capacitive strips, Fig. 8(a), is considered in TM polarization for $e\to 0$ and large $\ell=h-w$ values while the array of inductive strips, Fig. 8(b), is considered in TE polarization for $e\to 0$ and small $\ell=w$ values (namely, $w\ll h$ in both cases).

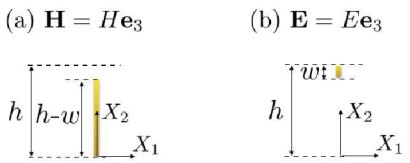

Figure 8. (a) Capacitive strips in TM polarization and (b) Inductive strips in TE polarization.

Results coming from transmission line theory in [14] give

- For TM polarization, the two sided impedance boundary condition reads

$$\begin{cases} E_2(0^+, X_2) = E_2(0^-, X_2) = Z^{\text{TM}} \, [\![H]\!] \,, \\ \text{with } Z^{\text{TM}} = -\dfrac{\mathrm{i}}{kh\mathcal{B}_0}. \end{cases} \tag{4.1}$$

- For TE polarization, the two sided impedance boundary condition reads

$$\begin{cases} E(0^+, X_2) = E(0^-, X_2) = Z^{\text{TE}} \, [\![H_2]\!] \,, \\ \text{with } Z^{\text{TE}} = \mathrm{i}kh\mathcal{B}_0/4. \end{cases} \tag{4.2}$$

Note that, in Ref. [14], $\alpha = kh\mathcal{B}_0/2$ is used (α is called the grid parameter for an electrically dense array of ideally conducting strips and has been obtained in [13]), leading to the usual forms $Z^{\text{TM}} = -\mathrm{i}/(2\alpha)$ and $Z^{\text{TE}} = \mathrm{i}\alpha/2$.

Now, we show that the conditions (4.1) and (4.2) are in agreement with the conditions obtained in our equivalent interface/surface model. In the TM polarization, for $e \to 0$ and owing to $\partial H/\partial X_1 = \mathrm{i}kE_2$, our jump conditions, Eqs. (3.2), simplify since $\mathcal{S}, \mathcal{C} \to 0$ and $\mathcal{B} \to \mathcal{B}_0$. It follows that $\partial H/\partial X_1$ (or equivalently E_2) is continuous across the interface and

$$[\![H]\!] = \mathrm{i}kh\mathcal{B}_0 E_2(0, X_2), \tag{4.3}$$

in agreement with Eq. (4.1). In the TE polarization, $e \to 0$ produces $\mathcal{C}_1 \simeq \mathcal{C}_2$. With $\partial E/\partial X_1 = -\mathrm{i}kH_2$, our boundary conditions Eqs. (3.7) simplify in

$$E(0, X_2) = -\mathrm{i}kh\mathcal{C} \, [\![H_2]\!] \,. \tag{4.4}$$

with E being continuous across the interface. This expression is in agreement with Eq. (4.2) if $\mathcal{C}_1(w) \simeq 4\mathcal{B}_0(\ell)$ (with $w = h - \ell$). This property is valid; we have calculated numerically $(\mathcal{C}_1, \mathcal{C}_2)$ for $w = h - \ell$ and $\ell \in [0.01;\ 0.99]$, and $e = 10^{-3}h$; we find $\mathcal{C}_1 = \mathcal{C}_2$ up to 0.1% and $C_1(w) = \mathcal{B}_0(\ell)/4$ up to 2%. In [14], this property is linked to the Babinet principle; a more definitive conclusion would require to introduce in our asymptotic model a scaling between our small parameter kh and the new small e/h.

(b) Comparison with the GSTCs

In a series of paper, Holloway and co workers presented the derivation of the so-called Generalized Sheet Transition Conditions (GSTCs) [12,15–18]. It is based on a formulation of the Maxwell equations in the sense of the distributions proposed in the 90s by Idemen [41] (note that an alternative derivation of the GSTCs has been proposed by the same authors using an homogenization technique, see *e.g.* [31]). Introducing fictitious magnetic charges and currents being described by Dirac delta functions concentrated on an interface, Idemen established jump conditions of the electric and magnetic fields across the interface expressed in terms of surface magnetic and electric polarization densities. In [15], these polarization densities are shown to be related to the mean value of the electric and magnetic fields at the interface, owing to the knowledge of two dyadics, called effective electric and magnetic polarizability densities χ^m and χ^e. The generalized transition conditions read

$$\begin{cases} \mathbf{e}_1 \times [\![\mathbf{H}]\!] = -\mathrm{i}\omega\chi^e \mathbf{E}_t^{av} - \mathbf{e}_1 \times \boldsymbol{\nabla}_{\mathbf{x}'} \left[\chi_1^m H_1^{av}\right], \\ [\![\mathbf{E}]\!] \times \mathbf{e}_1 = -\mathrm{i}\omega\chi^m \mathbf{H}_t^{av} + \mathbf{e}_1 \times \boldsymbol{\nabla}_{\mathbf{x}'} \left[\chi_1^e E_1^{av}\right]. \end{cases} \tag{4.5}$$

The quantities (E^{av}, H^{av}) corresponds to our definition $(\bar{E}, \bar{H})$, and we keep this latter notation in the following. In [12], the convention $e^{\mathrm{i}\omega t}$ while we use the convention $e^{-\mathrm{i}\omega t}$; this is why our Eq. (4.5) has $-\mathrm{i}\omega$ instead of $\mathrm{i}\omega$ in the Eqs. (1-2) of [12]. Also, we have simplified the notations (χ^e stands for χ_{ES},χ^m stands for χ_{MS}) and $(\chi_2^e, \chi_3^e, \chi_1^e)$ stand for $(\chi_{ES}^{xx}, \chi_{ES}^{yy}, \chi_{ES}^{zz})$ according to the direction of polarization of ($\mathbf{H}$ along $\mathbf{e}_3$ in the present paper, along y in these papers) and to the direction of the normal to the interface (along $\mathbf{e}_1$ in the present paper, along z in these papers).

As previously, we inspect the TM and TE cases.

- In TM polarization, $\mathbf{H}=(0,0,H)$ and $\partial H/\partial X_1 = \mathrm{i}\omega E_2$ (and $E_t = E_2$). The GSTCs simplify in

$$\begin{cases} [\![H]\!] = \chi_2^e \dfrac{\partial \bar{H}}{\partial X_1}(0,X_2), \\ \left[\!\left[\dfrac{\partial H}{\partial X_1}\right]\!\right] = \chi_3^m \dfrac{\partial^2 \bar{H}}{\partial X_1^2}(0,X_2) + \left(\chi_3^m + \chi_1^e\right) \dfrac{\partial^2 \bar{H}}{\partial X_2^2}(0,X_2), \end{cases} \tag{4.6}$$

where we have used that $\partial^2 H/\partial X_1^2 + \partial^2 H/\partial X_2^2 = -k^2 H$ (the Helmholtz equation). These conditions are less general that our Eqs. (2.16), but in agreement with the simplified forms Eqs. (3.2), written for inclusions being symmetric with respect to X_1. This is consistent with the assertion in [15] that the dyadics χ^e and χ^m are diagonal if the inclusions have sufficient symmetries. Our interface parameters are in this case simply linked to 3 of the 6 terms in χ^e and χ^m

$$\begin{cases} \chi_1^e = -h\mathcal{C} + h\mathcal{S}, \\ \chi_2^e = h\mathcal{B}, \\ \chi_3^m = -h\mathcal{S}. \end{cases} \tag{4.7}$$

- For TE polarization, the transition conditions, Eqs. (4.5), end up with

$$\begin{cases} [\![E]\!] = \chi_2^m \dfrac{\partial \bar{E}}{\partial X_1}(0,X_2), \\ \left[\!\left[\dfrac{\partial E}{\partial X_1}\right]\!\right] = \chi_3^e \dfrac{\partial^2 \bar{E}}{\partial X_1^2}(0,X_2) + \left(\chi_3^e + \chi_1^m\right) \dfrac{\partial^2 \bar{E}}{\partial X_2^2}(0,X_2), \end{cases} \tag{4.8}$$

which have the same forms as for TM polarization, by symmetry of the initial transition conditions for $(\mathbf{E},\mathbf{H})$ in Eqs. (4.5). We have used that $\mathbf{E}=(0,0,E)$ and the relations $\mathrm{i}\omega H_1 = \partial E/\partial X_2$, $\mathrm{i}\omega H_2 = -\partial E/\partial X_1$ (here $H_t = H_2$). It is a fundamental difference that the transition conditions are thought in the form of a discontinuity in the fields across the sheet since it does not allows easily to recover a boundary conditions, as in our Eqs. (2.31). Nevertheless, it is possible to find an equivalence. Specifically, if we impose

$$\chi_3^e = -\frac{2}{k^2 h(\mathcal{C}_1+\mathcal{C}_2)}, \quad \chi_1^m = 0, \quad \chi_2^m = 2h(\mathcal{C}_2 - \mathcal{C}_1), \tag{4.9}$$

the second equation in Eqs.(4.8) simplifies to $[\![\partial_{X_1} E]\!] = -k^2 \chi_3^e \bar{E}(0,X_2)$. Next, using $\bar{E}(0,X_2) = 1/2\left[E(0^+,X_2) + E(0^-,X_2)\right]$, Eqs. (4.8) can be written

$$\begin{cases} E(0^+,X_2) = \left[\dfrac{\chi_2^m}{4} - \dfrac{1}{k^2\chi_3^e}\right] \dfrac{\partial E}{\partial X_1}(0^+,X_2) + \left[\dfrac{\chi_2^m}{4} + \dfrac{1}{k^2\chi_3^e}\right] \dfrac{\partial E}{\partial X_1}(0^-,X_2), \\ E(0^-,X_2) = -\left[\dfrac{\chi_2^m}{4} - \dfrac{1}{k^2\chi_3^e}\right] \dfrac{\partial E}{\partial X_1}(0^+,X_2) - \left[\dfrac{\chi_2^m}{4} - \dfrac{1}{k^2\chi_3^e}\right] \dfrac{\partial E}{\partial X_1}(0^-,X_2), \end{cases} \tag{4.10}$$

and together with (4.9), we recover our effective boundary conditions Eqs. (2.31).

Thus, our approach recovers the GSTCs based on Idemen's formulation both in TM and TE polarizations in a simple geometry, and we have established the relations between the polarization densities and our interface parameters. We end this section with a remark concerning the GSTCs. The formulation of the GSTCs is fixed once and for all in the form of (4.5), and it is to our opinion the weakness of this formulation. Indeed, (4.5) is non adapted to some wave problems, and adapted is meant here robust to an inversion procedure as often used to retrieve the effective parameters. We illustrate this fact for Dirichlet inclusions (in TE polarization) comparing the results of retrieval procedures applied to the GSTCs and to our boundary conditions. In the

GSTCs, retrieval relations are established using Eqs. (3.9) and (4.9)

$$\begin{cases} F_1(\theta,k) = \dfrac{2}{\mathrm{i}k\cos\theta}\dfrac{T-1+R}{T+1+R} = \chi_3^e + (\chi_1^m + \chi_3^e)\tan^2\theta, \\ F_2(\theta,k) = \dfrac{2}{\mathrm{i}k\cos\theta}\dfrac{T-1-R}{T+1-R} = \chi_2^m. \end{cases} \tag{4.11}$$

These relations allow us to deduce $(\chi_1^m, \chi_2^m, \chi_3^e)$ from (R,T) being calculated numerically for various (θ,k). We checked that F_1 is linear in $\tan^2\theta$ and that F_2 is independent of θ; we also found that χ_2^m is frequency independent and that χ_3^e varies as $1/k^2$ as expected from (4.9). However, when reporting the retrieved parameters $(\chi_3^e, \chi_1^m, \chi_2^m)$, we observe divergences of χ_3^e and χ_1^m (Fig. 9(a)). Obviously, these divergences correspond to $R+T+1=0$, where the retrieval procedure applied to the GSTCs fails; unfortunately, Dirichlet inclusions produce $R\simeq -1$ and $T\simeq 0$ at the dominant order, thus vanishing values of $(R+T+1)$ are rather usual (in fact, the unusual situation is $R=1$ and $T=0$ which is accessible for High Impedance Surfaces, see *e.g.* [14]).

To the opposite, our effective boundary conditions (2.31) are robust to a retrieval method. With (R,T) given by Eqs. (3.9), the effective parameters $(\mathcal{C}_1, \mathcal{C}_2)$ can be deduced using

$$\begin{cases} \mathcal{C}_1 = \dfrac{1}{\mathrm{i}kh\cos\theta}\dfrac{2T}{T^2-(1-R)^2}, \\ \mathcal{C}_2 = \dfrac{1}{\mathrm{i}kh\cos\theta}\dfrac{1+T^2-R^2}{T^2-(1-R)^2}, \end{cases} \tag{4.12}$$

and with $R\simeq -1$, $T\simeq 0$ at the dominant order, we can anticipate that the inversion will be safe. From (R,T) calculated numerically, we checked that the two quantities in (4.12) are independent of θ and kh; next reporting the retrieved parameters $(\mathcal{C}_1, \mathcal{C}_2)$ (Fig. 9(b)), we observe that the retrieved parameters do not suffer from divergence. Besides, we also checked that the retrieved $(\mathcal{C}_1, \mathcal{C}_2)$ are in good agreement with the values given by the resolution of the elementary problems, Eqs. (2.29)-(2.30).

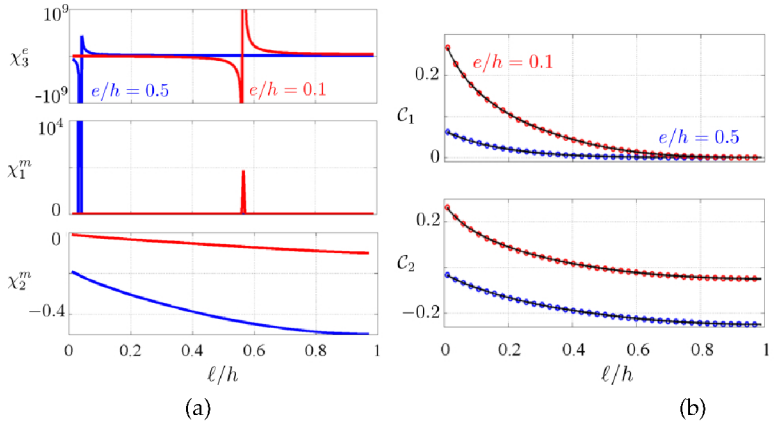

Figure 9. (a) Retrieved (χ^e, χ^m) for Dirichlet rectangular inclusions as a function of ℓ/h using a retrieval procedure on the GSTCs for e/h=0.1 and $e/h=0.5$; divergences of χ_3^e and χ_1^m are observed (b) Retrieved $(\mathcal{C}_1, \mathcal{C}_2)$ (open symbols) in the same conditions using a retrieval procedure on our jump conditions, (2.31); black lines show $(\mathcal{C}_1, \mathcal{C}_2)$ given by the direct resolution of the cell problems, Eqs. (2.29)-(2.30).

5. Conclusion

We have presented a two scale asymptotic method to derive effective boundary conditions of thin structured films. The problems ends with effective parameters characteristic of the film and which enter in boundary or jump conditions across an equivalent zero thickness interface. As in the classical homogenization, these parameters are obtained by the solutions of elementary problems. The method has been presented in the case of inclusions periodically located on a surface and associated to Neumann and Dirichlet boundary conditions. In electromagnetism, this corresponds to ideally conducting metallic inclusions in TM or TE polarization and it applies for two dimensional problems. In acoustics, this corresponds to sound hard or sound soft inclusions in three dimensional problems. The model has been validated in a simple scattering problem, an incident plane wave at oblique incidence on the film and it has been shown to be valid in the limit $kh, ke < 1$. While the former limit $kh < 1$ is expected for any homogenization theory, the condition $ke < 1$ defines a limiting thickness above which the classical homogenization should be efficient. In other words, classical homogenization applies for thick interfaces and our interface homogenization for thin interfaces, and thick and thin are measured by the wavelength.

We have shown that our interface conditions recovers the impedance boundary condition given by the transmission line theory for capacitive and inductive strips (that is for vanishing thickness inclusions and respectively large or small inclusions in the unit cell). Also, we have shown that the generalized sheet transition conditions are identical to our interface conditions for Neumann inclusions but significantly differ for Dirichlet inclusions. In this latter case, the formulation of the GSTCs is correct but it is not adapted to a retrieval procedure (the robustness of our interface conditions in a retrieval procedure is further discussed in Appendix A).

Direct extensions of the present study concern the case of penetrable inclusions (typically dielectric inclusions) and structured surfaces. Also, we have considered here the Helmholtz equation but more involved wave equations can be treated within the same formalism; we have in mind the Maxwell equations or the equations of elastodynamics. Finally, structurations involving resonances in the unit cell have been disregarded in the present paper. However, it is possible to adapt the method to account for them, as it has been done in classical homogenization.

Ethics statement. In this study, we have not conducted any experiments on human beings or animals, nor used any collection of human or animal data.

Data accessibility statement. This work does not have any experimental data.

Competing interests statement. We have no competing interests

Authors' contributions. Both authors have participated in the reflection on the problem, set up the formalism and they have written the paper.

Funding. J.-J. M is thankful for the support of the French AgenceNationale de la Recherche (ANR), under grant Aramis(ANR-12-BS01-0021) 'Analysis of Robust AsymptoticMethods In numerical Simulation in mechanics.' A.M. thanks the support of LABEX WIFI (Laboratory of Excellence within the French Program "Investments for the Future") under references ANR-10-LABX-24 and ANR-10-IDEX-0001-02 PSL*.

A. Interface parameters - Comparison with retrieved parameters

(a) Neumann boundary conditions for TM polarization

In an inverse procedure, as used in retrieval methods, (R, T) are measured experimentally or numerically, afterwards the retrieved parameters are deduced. To do that, from Eqs. (3.4), the

simplest procedure is to calculate

$$\begin{cases} F_1(\theta,k) = -\dfrac{2}{\mathrm{i}kh\cos\theta}\dfrac{T-1+R}{T+1+R} = \mathcal{S} + \mathcal{C}\tan^2\theta, \\ F_2(\theta,k) = \dfrac{2}{\mathrm{i}kh\cos\theta}\dfrac{T-1-R}{T+1-R} = \mathcal{B}, \end{cases} \tag{A 1}$$

for (R,T) calculated for various θ and k (with $kh, ke < 1$), to check that F_1 is linear with $\tan^2\theta$ and F_2 constant. If the case, then $(\mathcal{S},\mathcal{B},\mathcal{C})$ can be deduced. Fig. 10 show the results $\mathcal{S}$, $\mathcal{B}$ and $\mathcal{C}$ as a function of ℓ/h for various e/h. We get a good agreement between the retrieved parameters and the interface parameters coming from the elementary problems.

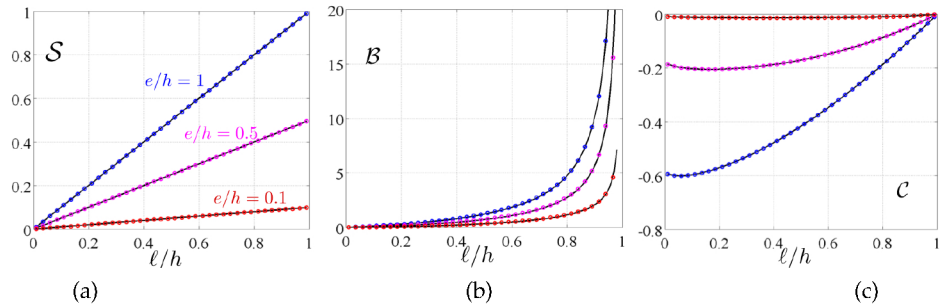

Figure 10. Effective parameters of rectangular Neumann inclusions $\mathcal{S}$, $\mathcal{B}$ and $\mathcal{C}$ as a function of ℓ/h for $e/h = 0.1$, 0.5 and 1. Black lines show the interface parameters given by homogenization, Eqs. (3.1) and symbols show the parameters obtained by retrieval method on (R,T).

The limit $\ell \to h$ produces a divergence in $\mathcal{B}$, according to Eq. (3.1). This leads in Eqs. (3.4) to $b \to \infty$ while a remains finite, thus, $R \to 1/(1+\mathrm{i}a)$ and $T \to -\mathrm{i}a/(1+\mathrm{i}a)$. Obviously, one would expect $R = 1$ and $T = 0$ in this case of reflecting wall. It is a classical problem in homogenization theories when a new small parameter is introduced, here $\varepsilon' = 1 - \ell/h$, and appropriate treatment should be done to treat this double limit. Amusingly, the problem does not appear if $e = 0$ in which case $a = 0$.

(b) Dirichlet boundary conditions for TE polarization

In terms of a retrieval procedure, $\mathcal{C}_1$ and $\mathcal{C}_2$ can be obtained owing to the inversion

$$\mathcal{C}_1 = \frac{1}{\mathrm{i}kh\cos\theta}\frac{2T}{T^2-(1-R)^2}, \mathcal{C}_2 = \frac{1}{\mathrm{i}kh\cos\theta}\frac{T^2+(1-R^2)}{T^2-(1-R)^2} \tag{A 2}$$

The behavior of the retrieved parameters are reported in Figs. 11, together with the interface parameters calculated in the elementary problem, Eqs. (3.5), and again a good agreement is observed.

For $e \to 0$ and $\ell \to 0$, $\mathcal{C}_1$ and $\mathcal{C}_2$ diverge (the divergence has logarithm behavior) with $\mathcal{C}_1 - \mathcal{C}_2 \to 0$. This implies $R \to 0$ and $T \to 1$, as expected. In this case, although this limit is outside the validity expected within the present analysis (c_1 and c_2 have been assumed small), we do not find unphysical limit.

For $\ell \to h$, $\mathcal{C}_1 \to 0$ and $\mathcal{C}_2 \to -e/2$; this is expected since the elementary problem for $e^{(+)}$ essentially reduces to a wall associated to Dirichlet boundary condition $e^{(+)}(e/2, y_2) = 0$, for which an exact solution is $e^{(+)}(y_1 > 0) = y_1 - e/2$. We get $T \to 0$ and $|R| \to 1$ with $R \sim -e^{\mathrm{i}k\cos\theta e}$, which is expected for a Dirichlet wall at $y_1 = e/2$. This limit does not suffer incompatibility with the assumption of small c_1 and c_2.

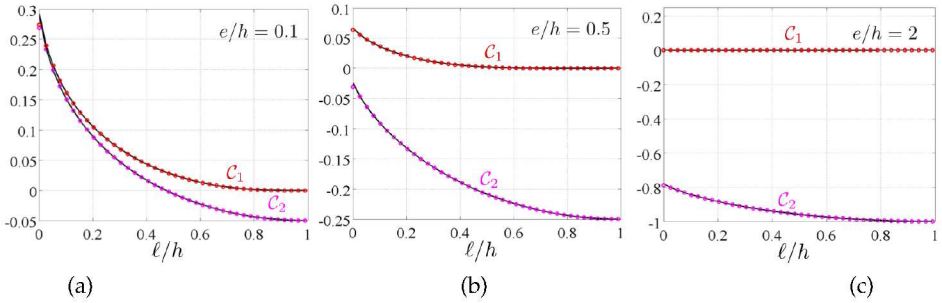

Figure 11. Effective parameters of rectangular Dirichlet inclusions $\mathcal{C}_1$ and $\mathcal{C}_2$ as a function of ℓ/h for $e/h = 0.1$, 0.5 and 2. Black lines show the interface parameters given by homogenization, Eqs. (3.5) and symbols show the retrieved parameters, Eqs. (A 2).

References

1. Felbacq D, Bouchitté G. 1997 Homogenization of a set of parallel fibres. *Waves in Random Media*, **7**(2), 245–256.
2. Căbuz A, Felbacq D, Cassagne D. 2007. Homogenization of negative-index composite metamaterials: A two-step approach. *Phys. Rev. Lett.* **98**(3), 037403.
3. Mercier JF, Cordero ML, Félix S, Ourir A, Maurel, A. 2015 Classical homogenization to analyse the dispersion relations of spoof plasmons with geometrical and compositional effects. *Proc. R. Soc. A* **471**, 20150472.
4. Bouchitté G, Felbacq D. 2004 Homogenization near resonances and artificial magnetism from dielectrics. *C R Mathématique* **5**, 377–382.
5. Felbacq D, Bouchitté G. 2005 Left-handed media and homogenization of photonic crystals *Optics letters* **30**, 1189–1191.
6. Vynck K, Felbacq D, Centeno E, Căbuz A, Cassagne D, Guizal I. 2009 All-dielectric rod-type metamaterials at optical frequencies, *Phys. Rev. Lett.* **102**(13), 133901.
7. Farhat M, Guenneau S, Enoch S, Movchan AB. 2009 Negative refraction, surface modes, and superlensing effect via homogenization near resonances for a finite array of split-ring resonators, *Phys Rev E* **80**(4), 046309.
8. Craster RV, Kaplunov J, Nolde E, Guenneau S. 2011. High-frequency homogenization for checkerboard structures: defect modes, ultrarefraction, and all-angle negative refraction. *JOSA A* **28**, 1032–1040.
9. Antonakakis T, Craster RV, Guenneau S. 2013 Asymptotics for metamaterials and photonic crystals. *Proc. R. Soc. A* **469**, 20120533.
10. Antonakakis T, Craster RV, Guenneau S., Skelton E.A. 2013 An asymptotics for waves guided by diffraction gratings or along microstructured surfaces . *Proc. R. Soc. A* **470**, 20130467.
11. Simovski CR. 2011 On electromagnetic characterization and homogenization of nanostructured metamaterials, *J. Optics* **13** 013001,
12. Holloway CL, Kuester EF, Dienstfrey A. 2011 Characterizing metasurfaces/metafilms: The connection between surface susceptibilities and effective material properties *Antennas and Wireless Propagation Letters, IEEE*, **10** 1507–1511
13. Tretyakov S. 2003 Analytical modeling in applied electromagnetics, Artech House
14. Luukkonen O, Simovski C, Granet G, Goussetis G, Lioubtchenko D, Räisänen AV, Tretyakov S. 2008 Simple and accurate analytical model of planar grids and high-impedance surfaces comprising metal strips or patches *Antennas and Propagation, IEEE Transactions on*, **56** 1624–1632,
15. Kuester EF, Mohamed M, Piket-May M, Holloway CL. 2003 Averaged transition conditions for electromagnetic fields at a metafilm *Antennas and Propagation, IEEE Transactions on*, **51** 2641–2651,
16. Holloway CL, Mohamed M, Kuester EF, Dienstfrey A. 2005 Reflection and transmission properties of a metafilm: With an application to a controllable surface composed of resonant particles *Electromagnetic Compatibility, IEEE Transactions on*, **47** 853–865
17. Holloway CL, Dienstfrey A, Kuester EF, O'Hara JF, Azad AK, Taylor AJ. 2009 A discussion

on the interpretation and characterization of metafilms/metasurfaces: The two-dimensional equivalent of metamaterials, *Metamaterials*, **3** 100-112
18. Kim S, Kuester EF, Holloway CL, Scher AD, Baker-Jarvis J. 2011 Boundary effects on the determination of metamaterial parameters from normal incidence reflection and transmission measurements *Antennas and Propagation, IEEE Transactions on*, **59** 2226–2240
19. Morits D, Simovski C. 2010 Electromagnetic characterization of planar and bulk metamaterials: A theoretical study, *Phys. Rev. B* **82**(16) 165114.
20. Morits D, Simovski C. 2012 Erratum: Electromagnetic characterization of planar and bulk metamaterials: A theoretical study [Phys. Rev. B 82, 165114 (2010)], *Phys. Rev. B* **85**(3) 039901.
21. Marigo JJ, Pideri C. 2011 The effective behavior of elastic bodies containing microcracks or microholes localized on a surface, *International Journal of Damage Mechanics*, 1056789511406914,
22. David M, Marigo JJ, Pideri C. 2012 Homogenized interface model describing inhomogeneities located on a surface, *Journal of Elasticity*, **109** 153–187.
23. Capdeville Y, Marigo JJ. 2007 Second order homogenization of the elastic wave equation for non-periodic layered media, *Geophysical Journal International*, **170** 823–838.
24. Capdeville Y, Guillot L, Marigo JJ. 2010 1-D non-periodic homogenization for the seismic wave equation *Geophysical Journal International* **181** 897–910,
25. Guillot L, Capdeville Y, Marigo JJ. 2010 2-D non-periodic homogenization of the elastic wave equation: SH case *Geophysical Journal International*, **182** 1438-1454.
26. Capdeville Y, Guillot L, Marigo JJ. 2010 2-d non-periodic homogenization to upscale elastic media for p–sv waves, *Geophysical Journal International*, **182**, 903–922,
27. Capdeville Y, Marigo JJ. 2013 A non-periodic two scale asymptotic method to take account of rough topographies for 2-D elastic wave propagation, *Geophysical Journal International*, **192** 163–189,
28. Bonnet-Bendhia AS, Drissi D, Gmati N. 2004 Simulation of muffler's transmission losses by a homogenized finite element method *J. Comp. Acoust.* **12** 447–474.
29. Delourme B, Haddar H, Joly P. 2012 Approximate models for wave propagation across thin periodic interfaces, *Journal de mathématiques pures et appliquées*, **98**, 28–71
30. Delourme B, Haddar H, Joly P. 2013 On the well-posedness, stability and accuracy of an asymptotic model for thin periodic interfaces in electromagnetic scattering problems *Mathematical Models and Methods in Applied Sciences*, **23** 2433–2464,
31. Holloway C.L., Kuester E.F., Dienstfrey A. 2014 A Homogenization Technique for Obtaining Generalized Sheet Transition Conditions for an Arbitrarily Shaped Coated-Wire Grating, *Radio Science*, **49**(10), 813-850.
32. Sanchez-Hubert J, Sanchez-Palencia E. 1982 Acoustic fluid flow through holes and permeability of perforated walls *J. Mathematical Analysis and Applications* **87**, 427–453,
33. Martin PA, Dalrymple RA. 1988 Scattering of long waves by cylindrical obstacles and gratings using matched asymptotic expansions, *J. Fluid Mech.* **188** 465–490.
34. Kakuno S, Oda K, Liu PLF. 1992 Scattering of water waves by vertical cylinders with a backwall, *Coastal Eng. Proc.*, **1**.
35. Bouchitté G., Petit R. 1989 On the concepts of a perfectly conducting material and of a perfectly conducting and infinitely thin screen, *Radio Sci.* **24** 1326.
36. Petit R., Bouchitté G., Tayeb G, Zolla F. 1991 Diffraction by one-dimensional or two-dimensional periodic arrays of conducting plates, *Proc. SPIE* **1545**, 3141.
37. Martin PA. 2014 On acoustic and electric Faraday cages, Proc. R. Soc. A, **470**, 20140344.
38. Flagg CN, Newman JN. 1971 Sway added-mass coefficients for rectangular profiles in shallow water, *J. Ship Res.*, **15**
39. Morse P, Ingard K. 1968 Theoretical acoustics, *Princeton university press*.
40. Marcuvitz N, Handbook MW. 1964 Radiation Lab Series No. 10, *Boston Technical Publishers, Lexington, MA*
41. Idemen M. 1990 Universal boundary relations of the electromagnetic field *J. Phys. Soc. Jap.* **59**, 71–80,